ROBUST POSTURE CONTROL OF A MOBILEWHEELED PENDULUM MOVING ON AN INCLINED PLANE

Danielle Sami Nasrallah[1†], Hannah Michalska[2†] and Jorge Angeles[1†]
[1]*Department of Mechanical Engineering,*
[2]*Department of Electrical and Computer Engineering,*
and [†]*Centre for Intelligent Machines*
McGill University, Montreal, Canada

Keywords: Wheeled Robots, Nonholonomy, Posture Control, Inclined Plane, Zero-Dynamics, Lyapunov Functions, Sliding Mode, Invariance, Parameters Uncertainties.

Abstract: The paper considers a specific class of wheeled mobile robots referred to as *mobile wheeled pendulums* (MWP). Robots pertaining to this class are composed of two wheels rotating about a central body. The main feature of the MWP pertains to the central body, which can rotate about the wheel axes. As such motion is undesirable, the problem of the *stabilization of the central body* in MWP is crucial. The novelty of the work presented here resides in the construction of a three-imbricated loop controller that delivers the full control strategy for the robot posture and copes with parameters uncertainties. Simulations on the performance of the controlled system are provided.

1 INTRODUCTION

This paper introduces a three-loop robust control scheme for controlling the posture of an anti-tilting outdoor mobile robot, ATOM, moving on an inclined plane. ATOM is composed of three rigid bodies: the central body, a cylinder whose center of mass is offset from its geometric center, and two spherical wheels rotating about the central body, as shown in Fig. 1. The system inputs are the two torques applied to the wheels. According to its structure, ATOM pertains to the class of Mobile Wheeled Pendulums (MWP). Many developments in the field of MWP have been reported recently: the US patent behind the Ginger and then the Segway Human Transporter projects (Kamen et al., 1999), JOE, a mobile inverted pendulum (Grassser et al., 2002), and, more recently, Quasimoro, a quasiholonomic mobile robot (Salerno and Angeles, 2004). A feature common to MWPs, that is not encountered in other wheeled robots, is that their central body, which constitutes the robot platform, can rotate about the wheels axis. This motion must not occur, leading to a new challenging problem for MWP which is the stabilization of the central body, aside the classical control problem due to nonholonomy. Therefore, although an intensive literature has dealt with the control of wheeled robots in the past (Campion et al., 1990; Samson and Abderrahim, 1999; Astolfi, 1994; Wit and Sordalen, 1992; Chwa, 2004; Guldner and Utkin, 1994), the control techniques reported there cannot be applied to MWP directly.

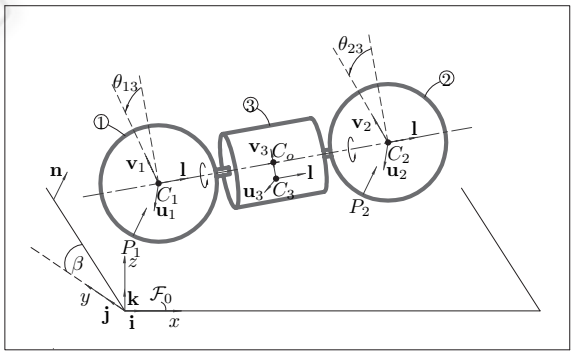

Figure 1: ATOM robot.

For example, any attempt to control the robot motion in conventional input-output mode results in unstable zero-dynamics, unless a friction torque is introduced between the central body and the wheels—such friction damps naturally the oscillation and eliminates trivially the serious issue of unstable zero-dynamics as it has been the case in (Grassser et al., 2002; Salerno and Angeles, 2004). (Pathak et al., 2005) were the first to attempt a solution to the

Sami Nasrallah D., Michalska H. and Angeles J. (2006).
ROBUST POSTURE CONTROL OF A MOBILEWHEELED PENDULUM MOVING ON AN INCLINED PLANE.
In *Proceedings of the Third International Conference on Informatics in Control, Automation and Robotics*, pages 34-41
DOI: 10.5220/0001213100340041

problem of the unstable zero-dynamics. This was done by introducing a two-layer controller. However, such stabilization of the central body is achieved only locally, i.e., for inclination angles of the central body near zero, as conventional linearization is employed. Moreover, the controller proposed there lacks robustness with respect to parameters uncertainties. Furthermore, most of the work done in the field of wheeled robots to date, including the references cited above, considers robots moving on a horizontal plane. In the light of previous contributions, the novelty of the work reported here is as outlined below:

1. To the best of the authors' knowledge, this is the first attempt to fully control the posture of a MWP-class robot moving on an inclined plane.
2. The posture control is achieved simultaneously with the stabilization of the central body, except that no restrictions on the central body inclination are considered, thus rendering the control proposed here global, and solving the unstable zero-dynamics problem regardless of the central body inclination. The control is accomplished by using a three-loop feedback structure with (i) the inner loop, based on input-output linearization, responsible for the stabilization of the central body and the control of the steering rate, (ii) the intermediate loop, based on an intrinsic dynamic property that is referred to as the *natural behavior of the system*, responsible for the control of the heading velocity, and (iii) the outer loop, based on sliding-mode control and Lyapunov functions for navigation, responsible for the posture control. It is noteworthy that after stabilizing the central body and controlling heading and steering velocities, the system becomes equivalent to any car-like robot, thus allowing the application of conventional techniques for position and orientation control. Therefore, the structure of the external loop is based on the work reported in (Guldner and Utkin, 1994), with an additional improvement to ensure smooth entering into the sliding mode.
3. It is shown that a special choice of the generalized coordinates (Euler-Rodrigues parameters, as opposed to Euler angles used in all the other references), combined with a particular selection of the system output functions in the inner loop, *globally linearizes* the dependence between the selected output variables of the inner loop and the forward acceleration of the robot. It is this feature that makes the approach outlined here more powerful than that of (Grassser et al., 2002; Salerno and Angeles, 2004; Pathak et al., 2005), as it eliminates the need to apply local linearization, rendering the technique completely global and nonlinear. Moreover, this linear dependance allows us to implement a linear controller for the intermediate loop, which, combined to the sliding-mode controller of the outer loop, renders the full control scheme less sensitive to parameters uncertainties.

The paper is organized in sections 2–4 below. In Section 2 we formulate the system state-space representation. In Section 3 we construct the three-loop controller. In Section 4 we present the simulation results confirming the expected performance of the controller.

2 MATHEMATICAL MODEL

The spherical shape of ATOM's wheels allows the robot to recover its posture after flipping over, thus rendering it anti-tilting. Moreover, the centers of mass of the wheels are assumed, by design, to coincide with the geometric centers of the spheres, while the center of mass of the central body is offset from its geometric center. The wheels are denoted bodies 1 and 2, while the central body is body 3, the symbols used for the robot modeling being summarized in Table 1. The Euler-Rodrigues parameters r_0 and $\mathbf{r}$ are used to

Table 1: List of Symbols.

b	Distance between the wheel centers
$\mathbf{c}_i$	Position vector of the center of mass C_i of the i^{th} body, $i = 1, 2, 3$
$\mathbf{c}_o$	Position vector of the geometric center C_o of the central body
d	Offset between the geometric center and the center of mass of the central body
$\{\mathbf{i}, \mathbf{j}, \mathbf{k}\}$	Right-handed orthogonal triad describing the orientation of the inertial frame $\mathcal{F}_0$
$\mathbf{l}$	Unit vector along the line of wheel centers, directed from C_1 to C_2
m_c	Mass of the central body
m_w	Mass of each wheel
$\mathbf{n}$	Unit vector normal to the inclined plane
r_w	Radius of each wheel
$r_0,\ \mathbf{r}$	Euler-Rodrigues parameters describing the orientation of the central body
$\{\mathbf{u}_i, \mathbf{l}, \mathbf{v}_i\}$	Right-handed orthogonal triad describing the orientation of the i^{th} body
$\mathbf{v}_3$	Unit vector directed from C_3 to C_o
$\mathbf{I}_c$	Inertia matrix of the central body
$\mathbf{I}_w$	Inertia matrix of each wheel
θ_{i3}	Angular displacement of the i^{th} wheel with respect to the central body
τ_i	Torque applied to the i^{th} wheel
$\boldsymbol{\omega}_i$	Angular velocity vector of the i^{th} body in $\mathcal{F}_0$

describe the orientation of body 3 in the inertial frame $\mathcal{F}_0$. In our previous work (Nasrallah et al., 2005), the mathematical model of ATOM moving on a general warped surface was developed. The terrain geometry enters the dynamics explicitly via the vectors normal to the ground at the contact points. Moreover, the particular case corresponding to the motion on an inclined plane is also included. Furthermore, in a more recent work (Nasrallah et al., 2006), we performed a model reduction that facilitates understanding the intrinsic dynamic properties of the system. Therefore, we present below the state-space formulation of the reduced model.

The six-dimensional vector of generalized coordinates $\mathbf{q}$ is defined as

$$\mathbf{q} = \begin{bmatrix} x_{\mathbf{c}_o} & y_{\mathbf{c}_o} & \mathbf{r}^T & r_0 \end{bmatrix}^T \quad (1)$$

while the three-dimensional vector of independent velocities is

$$\mathbf{v} = \begin{bmatrix} v_c & \omega_{3p} & \omega_{3l} \end{bmatrix}^T \quad (2)$$

where v_c is the heading velocity of the robot, namely,

$$v_c = \frac{r_w}{2}(\dot{\theta}_{13} + \dot{\theta}_{23} + 2\omega_{3l})$$

while ω_{3p} is the robot steering rate, given by

$$\omega_{3p} = \frac{r_w}{b}(\dot{\theta}_{13} - \dot{\theta}_{23})$$

and ω_{3l} is the projection along the line of (wheels) centers of $\boldsymbol{\omega}_3$, the angular velocity of the central body. The nine-dimensional state vector thus becomes

$$\mathbf{x}^T = \begin{bmatrix} \mathbf{q}^T & \mathbf{v}^T \end{bmatrix} \quad (3)$$

and the full state-space model of the system is, in turn,

$$\dot{\mathbf{x}} = \mathbf{f}(\mathbf{x}) + \mathbf{g}_p(r_0, \mathbf{r})\tau_p + \mathbf{g}_m(r_0, \mathbf{r})\tau_m \quad (4)$$

where

$$\mathbf{f}(\mathbf{x}) = \begin{bmatrix} v_c\, \mathbf{h}^T\mathbf{i} \\ v_c\, \mathbf{h}^T\mathbf{j} \\ (1/2)(r_0\mathbf{1} - \mathbf{R})(\omega_{3p}\mathbf{n} + \omega_{3l}\mathbf{l}) \\ -(1/2)\mathbf{r}^T(\omega_{3p}\mathbf{n} + \omega_{3l}\mathbf{l}) \\ \mathbf{f}_v \end{bmatrix}$$

while

$$\mathbf{g}_p = \begin{bmatrix} \mathbf{0}_6^T & \mathbf{g}_{v_p}^T \end{bmatrix}^T \text{ and } \mathbf{g}_m = \begin{bmatrix} \mathbf{0}_6^T & \mathbf{g}_{v_m}^T \end{bmatrix}^T$$

with

$$\mathbf{f}_v = \begin{bmatrix} r_w(F_b + F_c + G_b + G_c) \\ (2r_w/b)(F_a + G_a) \\ F_b + G_b \end{bmatrix}$$

and

$$\mathbf{g}_{v_p} = \begin{bmatrix} r_w J_d \\ 0 \\ -J_c \end{bmatrix}, \quad \mathbf{g}_{v_m} = \begin{bmatrix} 0 \\ (2r_w/b)J_a \\ 0 \end{bmatrix}$$

Moreover, $\mathbf{h}$ is a unit vector given by

$$\mathbf{h} = \mathbf{l} \times \mathbf{n}$$

while $\mathbf{R}$ is the cross-product matrix (CPM)[1] of vector $\mathbf{r}$, and $\mathbf{1}$ is the 3×3 identity matrix. Furthermore the input torques τ_1 and τ_2 have been transformed into τ_p and τ_m, as follows

$$\tau_p = \tau_1 + \tau_2 \text{ and } \tau_m = \tau_1 - \tau_2 \quad (5)$$

and

$$\begin{aligned}
F_a(r_0, \mathbf{r}, \mathbf{v}) &= J_a[-4C_d\omega_{3p}\omega_{3l} + (2/r_w)C_b\omega_{3p}v_c] \\
F_b(r_0, \mathbf{r}, \mathbf{v}) &= (J_c - J_b)(b/r_w)C_b({\omega_{3p}}^2 + {\omega_{3l}}^2) \\
&\quad + J_b(b/r_w)C_d{\omega_{3p}}^2 \\
F_c(r_0, \mathbf{r}, \mathbf{v}) &= -J_d(b/r_w)C_b({\omega_{3p}}^2 + {\omega_{3l}}^2) \\
&\quad - J_c(b/r_w)C_d{\omega_{3p}}^2 \\
G_a(r_0, \mathbf{r}) &= -2J_a m_c g d(r_w/b)(\mathbf{v}_3 \times \mathbf{n})^T\mathbf{k} \\
G_b(r_0, \mathbf{r}) &= (J_c - J_b)(2m_w + m_c)g r_w\ \mathbf{h}^T\mathbf{k} \\
&\quad + J_b m_c g d\ \mathbf{u}_3^T\mathbf{k} \\
G_c(r_0, \mathbf{r}) &= -J_c m_c g d\ \mathbf{u}_3^T\mathbf{k} - J_d(2m_w + m_c)g r_w\ \mathbf{h}^T\mathbf{k} \\
C_a(r_0, \mathbf{r}) &= m_c(r_w d^2/b)\mathbf{h}^T\mathbf{u}_3\ \mathbf{h}^T\mathbf{v}_3 \\
C_b(r_0, \mathbf{r}) &= m_c(r_w^2 d/b)\mathbf{h}^T\mathbf{v}_3 \\
C_c(r_0, \mathbf{r}) &= (r_w/b)(I_{cu} - I_{cv})\mathbf{h}^T\mathbf{u}_3\ \mathbf{h}^T\mathbf{v}_3 \\
C_d(r_0, \mathbf{r}) &= C_a + C_c \\
I_a &= 2(r_w/b)^2 I_{wu} + I_{wl} + m_w r_w^2 + m_c r_w^2/4 \\
I_b &= -2(r_w/b)^2 I_{wu} + m_c r_w^2/4 \\
I_c &= I_{wl} + m_w r_w^2 + m_c r_w^2/2 \\
I_d &= I_{cl} + m_c d^2 \\
I_e(r_0, \mathbf{r}) &= (r_w/b)^2[(I_{cu} + m_c d^2)\mathbf{h}^T{\mathbf{v}_3}^2 + I_{cv}\mathbf{h}^T{\mathbf{u}_3}^2] \\
I_f(r_0, \mathbf{r}) &= m_c(r_w d/2)\mathbf{h}^T\mathbf{u}_3 \\
J_a(r_0, \mathbf{r}) &= (1/2)/(I_a - I_b + 2I_e) \\
J_b(r_0, \mathbf{r}) &= I_c/(I_c I_d - 2{I_f}^2) \\
J_c(r_0, \mathbf{r}) &= (I_c - I_f)/(I_c I_d - 2{I_f}^2) \\
J_d(r_0, \mathbf{r}) &= (I_d/2 - I_f)/(I_c I_d - 2{I_f}^2)
\end{aligned}$$

3 POSTURE CONTROL

In this section we discuss posture control of ATOM as it moves on an inclined plane. This control objective must be achieved simultaneously with the stabilization of the central body in order to avoid unstable zero-dynamics. The controller introduced here has a triple-loop feedback structure, as shown in Fig. 2. The task of the inner loop is to control, via the system inputs τ_p and τ_m, two variables: (i) the steering rate

[1] The CPM of a vector $\mathbf{v} \in \mathbb{R}^3$ is defined, for every $\mathbf{x} \in \mathbb{R}^3$ as well, as $\mathbf{V} = \mathrm{CPM}(\mathbf{v}) = \partial(\mathbf{v} \times \mathbf{x})/\partial\mathbf{x}$

ω_{3p}, and (ii) a function of the system outputs. It is worth noticing that this function is chosen judiciously in order to stabilize the central body and to provide a linear dependence with the heading acceleration $\dot{v}_c$. Then, the task of the intermediate loop is to control the heading velocity v_c, while the task of the outer loop is to control the robot position and orientation via v_c and ω_{3p} using sliding mode control with Lyapunov function for navigation. Note that the intermediate loop benefits of an intrinsic dynamical property that is referred to as the *natural behavior of the system* and was introduced in a previous work (Nasrallah et al., 2006). In the present work, we will employ that property.

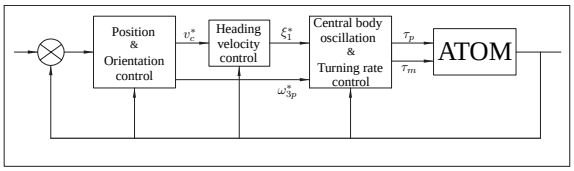

Figure 2: The block diagram of the robot and its associated control scheme.

The triple-loop controller is designed in sections 1–6 below. In Section 1 we introduce the normal form leading to the input-output linearization of the system. In Section 2 we synthesize the inner-loop. In Section 3 we derive the explicit relation between the heading acceleration and the output function of the inner loop. In Section 4 we synthesize the intermediate loop. In Section 5 we define the Lyapunov function for navigation and the sliding surface that will be used for posture control and synthesize the outer-loop. In Sections 6 and 7 we analyze the system stability and the zero-dynamics.

3.1 Normal Form

The well-known notions of *vector relative degree* and *normal form* (Sastry, 1999) are the essential tools in input-output linearization. The normal form is displayed here, while omitting the intermediate calculations for the sake of brevity. These calculations are preceded by the determination of the dimension of the largest linearizable subsystem, following the methods suggested in (Marino, 1986). As it turns out, the dimension of the largest linearizable subsystem of ATOM is four (Nasrallah et al., 2006). Therefore, the output functions of the system, whose relative degree must not exceed four, are chosen so as to secure the control over the oscillations of the central body as well as the robot turning rate. The specific form of the first output function ξ_1 involves a thorough analysis of the dependence of the output upon the heading acceleration of the robot. Specifically, the construction employs the additional requirement that the function ξ_1 be chosen to be linear with respect to the heading acceleration of the robot. The outputs are hence proposed to be

$$\begin{aligned}\xi_1(\mathbf{x}) &= \mathbf{u}_3^T\mathbf{k}\\ \xi_2(\mathbf{x}) &= \dot{\xi}_1 = \dot{\mathbf{u}}_3^T\mathbf{k} = \mathbf{u}_3^T(\mathbf{k}\times\mathbf{n})\,\omega_{3p} - \mathbf{v}_3^T\mathbf{k}\,\omega_{3l}\\ \xi_3(\mathbf{x}) &= \omega_{3p}\end{aligned} \tag{6}$$

To complete the coordinate system, six more transformation functions $\eta_i(\mathbf{x})$ are constructed. The distribution spanned by $\mathbf{g}_p$ and $\mathbf{g}_m$ being involutive, those distributions are constructed by requiring that:

$$\frac{\partial\eta_i}{\partial\mathbf{x}}^T\,\mathbf{g}_j(\mathbf{x}) = 0,\quad j=1,2,\quad 1\le i\le 6$$

Consequently,

$$\begin{aligned}\eta_1(\mathbf{x}) &= x_{\mathbf{c}_o} & \eta_4(\mathbf{x}) &= \mathbf{h}^T\mathbf{i}\\ \eta_2(\mathbf{x}) &= y_{\mathbf{c}_o} & \eta_5(\mathbf{x}) &= \mathbf{l}^T\mathbf{i}\\ \eta_3(\mathbf{x}) &= \mathbf{v}_3^T\mathbf{k} & \eta_6(\mathbf{x}) &= J_c v_c + r_w J_d\omega_{3l}\end{aligned}$$

It is straightforward to demonstrate that $\dot{\xi}_1$ as well as $\dot{\eta}_i$, for $i=1,\ldots,6$, do not depend on the input torques. Indeed, τ_p and τ_m act directly on $\dot{\xi}_2$ and $\dot{\xi}_3$, as shown below:

$$\begin{aligned}\dot{\xi}_2(\mathbf{x}) &= d_1 + (2r_w/b)J_a\mathbf{u}_3^T(\mathbf{k}\times\mathbf{n})\,\tau_m + J_c\mathbf{v}_3^T\mathbf{k}\,\tau_p\\ \dot{\xi}_3(\mathbf{x}) &= d_2 + (2r_w/b)J_a\tau_m\end{aligned} \tag{7}$$

where d_1 and d_2 represent the system drift terms, namely,

$$\begin{aligned}d_1 = {}& \dot{\mathbf{u}}_3^T(\mathbf{k}\times\mathbf{n})\,\omega_{3p} - \dot{\mathbf{v}}_3^T\mathbf{k}\,\omega_{3l} - \mathbf{v}_3^T\mathbf{k}\,(F_b+G_b)\\ &+(2r_w/b)\mathbf{u}_3^T(\mathbf{k}\times\mathbf{n})\,(F_a+G_a)\\ d_2 = {}& (2r_w/b)(F_a+G_a)\end{aligned}$$

3.2 Inner-Loop

Let ξ_1^* and ξ_3^* denote the reference values for ξ_1 and ξ_3, respectively. Adopting a second- and first- order system for the error dynamics of ξ_1 and ξ_3, respectively, yields:

$$\begin{aligned}\dot{\xi}_2 + k_2\,\xi_2 + k_1(\xi_1-\xi_1^*) &= 0\\ \dot{\xi}_3 + k_3(\xi_3-\xi_3^*) &= 0\end{aligned}$$

which, by virtue of eq. (7), implies:

$$\tau_m = -\frac{d_2 + k_3(\xi_3-\xi_3^*)}{(2r_w/b)J_a} \tag{8}$$

and

$$\tau_p = -\frac{d_1 + (2r_w/b)J_a\mathbf{u}_3^T(\mathbf{k}\times\mathbf{n})\tau_m + k_2\,\xi_2 + k_1(\xi_1-\xi_1^*)}{J_c\;\mathbf{v}_3^T\mathbf{k}} \tag{9}$$

Consequently,

$$\tau_1 = \frac{\tau_p+\tau_m}{2},\quad \tau_2 = \frac{\tau_p-\tau_m}{2}$$

3.3 Relation between $\dot{v}_c$ and $\mathbf{u}_3^T\mathbf{k}$

From eq. (4) the forward acceleration $\dot{v}_c$ is

$$\dot{v}_c = r_w(F_b + F_c + G_b + G_c) + r_w J_d \tau_p$$

When the internal loop reaches its steady-state, i.e., ξ_1 and ξ_3 reach their associated reference values, ξ_2, the first-order time-derivatives of ξ_1, vanishes; similarly, ω_{3p} and ω_{3l} vanish as well, thereby leading to

$$F_a = 0,\ F_b = 0,\ F_c = 0$$

and

$$\tau_p = \frac{G_b}{J_c},\ \tau_m = -\frac{G_a}{J_a}$$

Thus, the acceleration in the steady-state is

$$\dot{v}_{c_{ss}} = r_w \left(G_b + G_c + \frac{J_d}{J_c} G_b \right)$$

which, after simplification, becomes

$$\dot{v}_{c_{ss}} = d_3 + k_a\, \mathbf{u}_3^T\mathbf{k} = d_3 + k_a\, \xi_1 \qquad (10)$$

where

$$d_3 = -\frac{(2m_w + m_c) g r_w^2}{2(I_c - I_f)}\ \mathbf{h}^T\mathbf{k}$$

and

$$k_a = \frac{m_c g r_w d}{2(I_c - I_f)}$$

Equation (10) shows the possibility of controlling the heading velocity of the robot via the output function ξ_1, which represents the inclination of the central body. Moreover, the linear form of ξ_1 with respect to the heading acceleration delivers *global stabilization of the central body*.

3.4 Intermediate-Loop

Let v_c^* denote the reference value for the forward velocity. After compensation of the drift d_3, the transfer function of the intermediate closed loop in the Laplace domain becomes

$$\frac{V_c(s)}{V_c^*(s)} = \frac{(k_a/s)\, C(s)}{1 + (k_a/s)\, C(s)}$$

where $C(s)$, the controller transfer function, has the simple structure of a first-order system, namely, $k_v/(1 + \tau_v s)$. Thus,

$$\xi_1^* = -\frac{d_3}{k_a} + L^{-1}[C(s)(V_c^*(s) - V_c(s))] \qquad (11)$$

where L^{-1} denotes the inverse Laplace transformation.
Moreover, knowing that $|\mathbf{u}_3^T\mathbf{k}|$ is bounded by 1, the value of ξ_1^* is to be restricted to $[-1, 1]$. However, since $\mathbf{v}_3^T\mathbf{k}$ vanishes at the boundaries, this interval is further restricted to [-0.99,0.99].

3.5 Outer-Loop

Once the inner and intermediate loops are implemented, the system (ATOM + two internal control loops) is equivalent to any car-like robot, since the platform is stabilized and the new control inputs are v_c and ω_{3p}, the heading and steering velocities, respectively. For the construction of the position and orientation controller, the technique introduced in (Guldner and Utkin, 1994) is applied. It is based on sliding-mode control with Lyapunov function, as applied to a navigation problem and is additionally enhanced by a feature allowing smooth entry into the sliding mode. The central idea is to ensure that vector $\mathbf{h}$ is linearly dependent with a vector $\boldsymbol{\epsilon}$, which is defined as the gradient of the chosen Lyapunov function. When linear dependency is achieved, the system enters the sliding mode. The foregoing linear dependence condition does not require any switching, which guarantees that the distance between the current position of the system and the sliding surface decreases monotonically.
Finally, without loss of generality, the origin of the workspace is located at the goal posture and oriented in such a way that the line of wheel centers is parallel to the one of steepest ascent and the line joining the center of mass of the central body to its geometric center is normal to the plane. Therefore the reference values for the posture controller are:

$$x_{\mathbf{c}_o} = 0, \quad y_{\mathbf{c}_o} = 0 \quad \text{and} \quad |\mathbf{u}_3^T\mathbf{k}| = 1$$

Let $\mathbf{s}$ be the direction of steepest ascent of the inclined plane, i.e.,

$$\mathbf{s} = \mathbf{n} \times \mathbf{i}$$

Then the x and y coordinates of $\dot{\mathbf{c}}_o$ can be written as

$$\dot{x}_{c_o} = v_c\ \mathbf{h}^T\mathbf{i} \ \text{ and } \ \dot{y}_{c_o} = v_c \cos\beta\ \mathbf{h}^T\mathbf{s}$$

where β represents the inclination of the plane.
The Lyapunov function V for the navigation problem is chosen as

$$V(x_{c_o}, y_{c_o}) = \frac{1}{2}\left[\frac{x_{\mathbf{c}_o}^2}{2} + y_{\mathbf{c}_o}^2\right]$$

so that $\boldsymbol{\epsilon}$ is defined by

$$\boldsymbol{\epsilon}(x_{c_o}, y_{c_o}) = -\mathrm{grad}\,(V) = \begin{bmatrix} \epsilon_x \\ \epsilon_y \end{bmatrix}^T = \begin{bmatrix} -x_{\mathbf{c}_o}/2 \\ -y_{\mathbf{c}_o} \end{bmatrix}^T$$

Therefore, the equation of the sliding surface becomes

$$\Delta(\mathbf{q}) = \det \begin{bmatrix} \mathbf{h}^T\mathbf{i} & \epsilon_x/\|\boldsymbol{\epsilon}\| \\ \mathbf{h}^T\mathbf{s} & \epsilon_y/\|\boldsymbol{\epsilon}\| \end{bmatrix} = 0 \qquad (12)$$

where $\|\boldsymbol{\epsilon}\|$ denotes the Euclidian norm of $\boldsymbol{\epsilon}$.
Differentiating Δ with respect to time leads to

$$\dot{\Delta} = -D_1(\mathbf{q})\ \omega_{3p} + D_2(\mathbf{q})\ v_c$$

where

$$D_1(\mathbf{q}) = \mathbf{h}^T\mathbf{i}\ \frac{\epsilon_x}{\|\boldsymbol{\epsilon}\|} + \mathbf{h}^T\mathbf{s}\ \frac{\epsilon_y}{\|\boldsymbol{\epsilon}\|}$$

and

$$D_2(\mathbf{q}) = \frac{x_{\mathbf{c}_o} y_{\mathbf{c}_o}}{4\|\boldsymbol{\epsilon}\|^3}\left(\mathbf{h}^T\mathbf{i}^2 - 2\cos\beta\mathbf{h}^T\mathbf{s}^2\right) \frac{\mathbf{h}^T\mathbf{i}\ \mathbf{h}^T\mathbf{s}}{4\|\boldsymbol{\epsilon}\|^3}\left(-\cos\beta x_{\mathbf{c}_o}^2 + 2y_{\mathbf{c}_o}^2\right)$$

Convergence of Δ to zero within finite time can be achieved by imposing

$$\dot{\Delta} = -\zeta\sqrt{|\Delta|}\mathrm{sign}(\Delta) \ \text{ with } \ \zeta \geq 0$$

leading to

$$\xi_3^* = \omega_{3p}^* = \frac{1}{D_1}\left(D_2\, v_c + \zeta\sqrt{|\Delta|}\mathrm{sgn}(\Delta)\right) \quad (13)$$

Finally, introducing a positive scalar v_0 as an auxiliary control input yields

$$v_c^* = \|\boldsymbol{\epsilon}\| v_0\, \mathrm{sgn}(\mathbf{h}^T\mathbf{i}\,\epsilon_x) \quad (14)$$

Therefore, eqs. (8), (9), (11), (13), and (14) constitute the controller as implemented in three loops.

3.6 Analysis of the Stability

Equation (12) implies $\mathbf{h}^T\mathbf{i} = \pm\epsilon_x/\|\boldsymbol{\epsilon}\|$. Considering the positive case

$$\dot{x}_{c_o} = v_c\,\mathbf{h}^T\mathbf{i} = v_c\,\epsilon_x/\|\boldsymbol{\epsilon}\| = v_0\,\|\boldsymbol{\epsilon}\|$$
$$\dot{y}_{c_o} = v_c\cos\beta\,\mathbf{h}^T\mathbf{i} = v_c\cos\beta\,\epsilon_y/\|\boldsymbol{\epsilon}\| = v_0\,\cos\beta\,\epsilon_y$$

Thus,

$$\dot{V} = -\boldsymbol{\epsilon}^T\begin{bmatrix}\dot{x}_{c_o}\\ \dot{y}_{c_o}\end{bmatrix} = -\epsilon_x^2\, v_0 - \epsilon_y^2\,\cos\beta\, v_0 \ \leq 0$$

The same reasoning is employed for the negative case, thus ensuring system stabilization by standard Lyapunov asymptotic stability theory.

3.7 Analysis of the Zero-Dynamics

The zero-dynamics of the system is calculated by determining initial conditions and inputs such that the output of the system remains zero for all the time (Nasrallah et al., 2005). If the initial posture with the state $\mathbf{x}_0$ is such that the line of wheel centers is parallel to the direction of steepest ascent, and the line joining the center of mass of the central body to its geometric center is perpendicular to the plane, then it is a simple matter to verify that the zero dynamics is described by

$$\dot{\eta}_1 = v_{c_0} \ \text{ and } \ \dot{\eta}_i = 0 \ \text{ for } \ i = 2\ldots 6$$

Here, v_{c_0}, the initial heading velocity, decreases to zero because of the action of the outer-loop controller, which secures stable zero-dynamics.

4 SIMULATION RESULTS

In this section we present the simulation results for the closed-loop system. The inclination of the plane is of 30% for all the simulations. ATOM succeeds to reach the origin at the desired orientation starting from distinct initial conditions. Below we display four examples:

1. coming from up right, Fig. 4(a)

$$x_{c_o} = 1\ ,\ \ y_{c_o} = 1 \ \text{ and } \ \mathbf{u}_3^T\mathbf{i} = -\sqrt{2}/2$$

2. coming from up left, Fig. 4(b)

$$x_{c_o} = -2\ ,\ \ y_{c_o} = 2 \ \text{ and } \ \mathbf{u}_3^T\mathbf{i} = -\sqrt{2}/2$$

3. coming from down right, Fig. 4(c)

$$x_{c_o} = 2\ ,\ \ y_{c_o} = -7 \ \text{ and } \ \mathbf{u}_3^T\mathbf{i} = 0$$

4. coming from down left, Fig. 4(d)

$$x_{c_o} = 1\ ,\ \ y_{c_o} = 1 \ \text{ and } \ \mathbf{u}_3^T\mathbf{i} = -\sqrt{2}/2$$

Furthermore, we test the controller performance versus the parameter uncertainties. We recall here that the controller is composed of three-imbricated loops. The inner loop, based on input-output linearization, is obviously dependent of the robot parameters. As for the intermediate loop, the judicious choice of the function ξ_1 allowed a linear dependence between the heading acceleration of the robot and this function. Therefore, we were able to implement a linear controller $C(s)$, with constant parameters. For the outer loop the choice of the sliding-mode control and the auxiliary constant input v_0 rendered the controller less dependent of the system parameters. Note that the choice of the controller parameters was not a simple task since the system itself is nonsymmetric, due to the *up* and *down* motion of ATOM on the inclined plane. Therefore, we show two simulations of ATOM moving on the same inclined plane with a slope of 30%, except that the robot and terrain parameters seen by the controller are over- and underestimated, respectively. The error on the normal vector to the ground is of 10%, while the error on the moments of inertia of the rigid bodies composing the robot and the offset d between the geometric and center of mass are of 20%. In both cases, i.e., under- and over-estimation, ATOM succeeds to reach the origin with the desired orientation, which can be verified by looking to the evolution in time of the $x-$, $y-$, and $z-$ components of C_o depicted in Fig. 4(a). The time history of the signals v_c, ω_{3p}, and ξ_1 are displayed in Fig. 4(b), (c), and (d), respectively. The torques applied to the wheels in Fig.5.

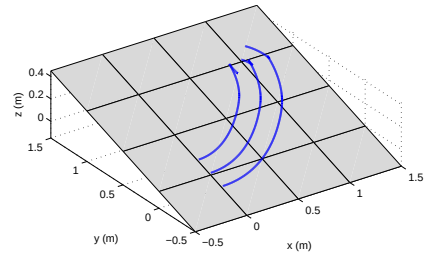

(a)

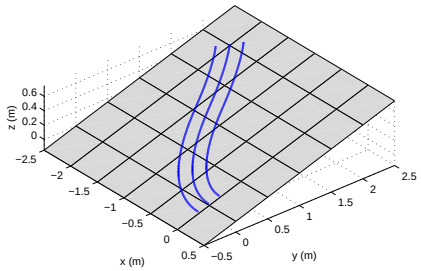

(b)

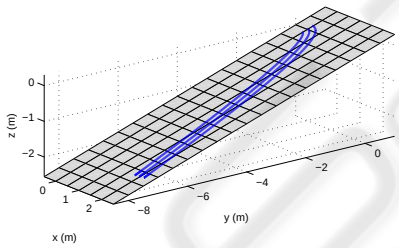

(c)

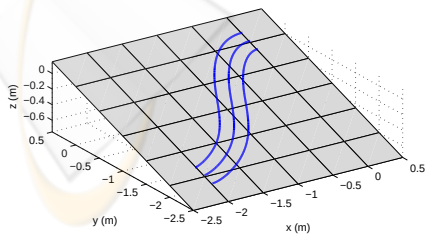

(d)

Figure 3: Manoeuvres performed by ATOM on the inclined plane: reaching the origin at the desired orientation from (a) up right; (b) up left; (c) down right; and (d) down left.

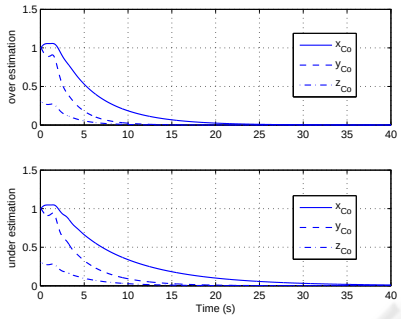

(a)

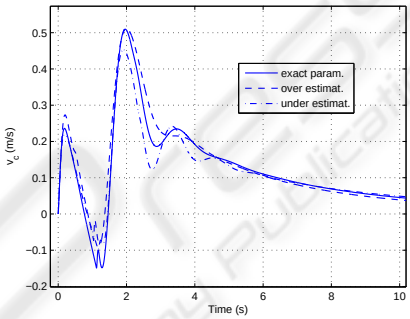

(b)

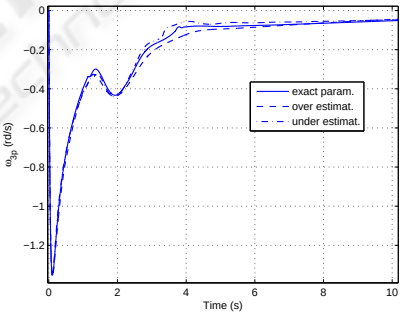

(c)

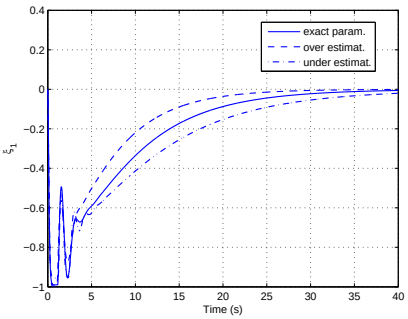

(d)

Figure 4: Controller performance versus parameters uncertainties: time-history of: (a) the $x-$, $y-$, and $z-$ components of C_o; (b) v_c; (c) ω_{3p}; and (d) ξ_1.

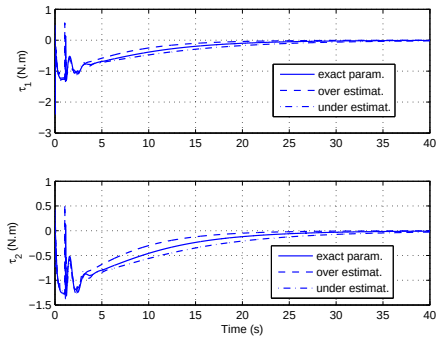

(a)

Figure 5: Controller performance versus parameters uncertainties: time history of τ_1 and τ_2.

5 CONCLUSION

The work reported here delivers a robust posture controller for a MWP-class robot moving on an inclined plane. The challenging issue in this design is to be able to control the posture of the robot simultaneously while stabilizing of the central body, which results in the absence of friction. Unlike previous attempts to control such systems, our controller is global and less sensitive to errors in the parameters estimation. We show that deep insight into the internal dynamics of the system, in conjunction with proper selection of a coordinate system and the system output function, are instrumental in the construction of feedback controllers for nonholonomic systems underlying unstable zero-dynamics.
Future work will focus on generalization of the motion of the robot to a warped, smooth surface.

ACKNOWLEDGEMENTS

This work was made possible by NSERC (Canada's Natural Sciences and Engineering Research Council) Grant OGP4532.

REFERENCES

D. L. Kamen, R. R. Ambrogi, R. J. Duggan, R. K. Heinzmann, B. R. Key, A. Skoskiewicz, P. K. Kristal, 1999, "Transportation Vehicles and Methods", US patent 5,971,091.

F. Grassser, A. D'Arrigo, S. Colombi and A. C. Rufer, 2002, "JOE: A Mobile, Inverted Pendulum", *IEEE Trans. Industrial Electronics* 49, No. 1, pp. 107-114.

A. Salerno and J. Angeles, 2004, "The Control of Semi-Autonomous Self-Balancing Two-Wheeled Quasi-holonomic Mobile Robots", *Proc. 15th CISM-IFToMM Symposium on Robot Design, Dynamics and Control (RoManSy)*, Montreal, June 14-18.

G. Campion, B. d'Andrea-Novel and G. Bastin, 1990, "Controllability and State Feedback Stabilizability of Non Holonomic Mechanical Systems", Advanced Robot Control, *Proc. of the International Workshop on Nonlinear and Adaptive and Control, Issues in Robotics*, Grenoble, November 21-23

C. Samson, K. Ait-Abderrahim, 1999, "Mobile Robot Control Part 1: Feedback Control of a Nonholonomic Wheeled Cart in Cartesian Space", INRIA, *Rapport de Recherche*, No.1288, October.

A. Astolfi, 1994, "On the Stabilization of Nonholonomic Systems", *Proc. 33rd Conference on Decision and Control*, Lake Buena Vista, December 14-16, pp. 3481-3486.

C. Canudas de Wit, O. J. Sordalen, 1992, "Exponential Stabilization of Mobile Robots with Nonholonomic Constraints", *IEEE Trans. Automatic Control* 37, No. 11, pp. 1791-1797.

D. Chwa, 2004, "Sliding-Mode Tracking Control of Nonholonomic Wheeled Mobile Robots in Polar Coordinates", *IEEE Trans. Control Systems Technology* 12, No. 4, pp. 637-644.

J. Guldner, V. I. Utkin, 1994, "Stabilization of Nonholonomic Mobile Robots Using Lyapunov Functions for Navigation and Sliding Mode Control", *Proc. 33rd Conference on Decision and Control*, Lake Buena Vista, December 14-16, pp. 2967-2972.

K. Pathak, J. Franch and S. K. Agrawal, 2005, "Velocity and Position Control of a Wheeled Inverted Pendulum by Partial Feedback Linearization", *IEEE Trans. Robotics* 21, No. 3, pp. 505-513.

D. S. Nasrallah, J. Angeles and H. Michalska, 2005, "Modeling of an Anti-Tilting Outdoor Mobile Robot", *ASME Proc. 5th International Conference on Mutlibody Systems, Nonlinear Dynamics, and Control*, Long Beach, September 25-28.

D. S. Nasrallah, J. Angeles and H. Michalska, 2006, "Velocity and Orientation Control of an Anti-Tilting Mobile Robot Moving on an Inclined Plane", *IEEE Proc. International Conference on Robotics and Automation*, Orlando, May 15-19, pp. 3717-3723.

S. Sastry, 1999, *Nonlinear Systems: Analysis, Stability, and Control*, Springer-Verlag.

R. Marino, 1986, "On the largest feedback linearizable subsystem", *Systems and Control Letters* 6, pp. 345–351.

D.S. Nasrallah, J. Angeles and H. Michaslka, 2006, "The Largest Feedback-Linearizable Subsystem of a Class of Wheeled Robots Moving on an Inclined Plane", to appear in *Proc. 16th CISM-IFToMM Symposium on Robot Design, Dynamics and Control (RoManSy)*, Warsaw, June 20-24.